Atomic spatial coherence with spontaneous emission in a strong-coupling cavity

Zhen Fang, Rui Guo, Xiaoji Zhou,* and Xuzong Chen
School of Electronics Engineering and Computer Science, Peking University, Beijing 100871, China
(Received 24 September 2009; published 20 July 2010)

The role of spontaneous emission in the interaction between a two-level atom and a pumped microcavity in the strong-coupling regime is discussed. In particular, using a quantum Monte Carlo simulation, we investigate atomic spatial coherence. It is found that atomic spontaneous emission destroys the coherence between neighboring lattice sites, while cavity decay does not. Furthermore, our computation of the spatial coherence function shows that the in-site locality is little affected by the cavity decay but greatly depends on the cavity pump amplitude.

DOI: 10.1103/PhysRevA.82.015601 PACS number(s): 03.75.Gg, 24.10.Lx, 37.30.+i

The combination of cold-atom physics and cavity quantum electrodynamics (QED) has made possible the investigation of the coherence properties of matter waves in periodic potentials [1–11]. A tunable optical lattice can be generated by pumping a single-mode microcavity with a far-detuned laser, and strong coupling between the atom(s) and the cavity field can be reached. In this regime the recoil by scattering photons can be very important [12,13]. Even a single photon may transfer significant momentum to the atom(s) and, in reverse, the atomic distribution also strongly affects the cavity field [2]. Cavity QED systems have been widely used in many fields, such as cavity cooling [3–6], atomic dynamics detection [7], or atomic quantum phase probing [8,9].

For the system of an ultracold atom in a strong-coupling cavity, the condition of large atomic detuning is often satisfied, which allows the influence of the atomic spontaneous emission to be neglected. However, when the long-time evolution or the steady-state properties of the system are being investigated, spontaneous emission can have a notable effect on the atomic spatial coherence and can no longer be neglected. The recoil by spontaneously emitted photons in random directions destroys the atomic spatial coherence, and interference fringes in momentum space may not be observed experimentally. Moreover, when coherently pumped by a laser field, the number of photons in the cavity grows rapidly and the cavity field experiences great fluctuation. The approximation of taking the lowest vibrational state in the Wannier expansion is no longer valid [10,11]. Thus, a fully quantum-mechanical model has to be implemented to describe the cavity QED system, and the Monte Carlo wave function (MCWF) method is commonly used to simulate the time evolution of such a system [14–17].

In this paper, the effect of spontaneous emission on the atomic coherence property in the cavity is studied with a fully quantum-mechanical model. By comparing the time evolution of the atomic momentum distribution with and without atomic spontaneous emission, we find that the influence of the atomic spontaneous emission cannot be neglected in evaluating the steady-state properties and is responsible for the loss of spatial coherence. Furthermore, the dependence of the atomic spatial coherence property on the cavity parameters is studied. The pumping strength rather than the cavity decay rate is the dominating factor affecting the atomic locality.

We consider a two-level atom with mass μ and transition frequency ω_a coupled to a single-mode standing-wave cavity with resonance frequency ω_c and mode function $f(\hat{\mathbf{r}})$ (see Fig. 1). The coupling strength between the atom and the cavity field is g. The cavity is pumped coherently by a laser with frequency ω_p and amplitude η. The photons can either leak out of the cavity from the end mirrors directly (cavity decay) or be emitted out of the cavity by the atom (spontaneous emission decay), with decay rates 2κ and 2γ, respectively. The time evolution of the system is governed by the master equation [18]

$$\dot{\rho} = \frac{1}{i\hbar}[H,\rho] + \mathcal{L}\rho. \tag{1}$$

Using the rotating-wave and electric-dipole approximations, the Hamiltonian can be depicted in the frame rotating with ω_p as [19,20]

$$\begin{aligned} H = &-\hbar\Delta_c\hat{a}^\dagger\hat{a} - i\hbar\eta(\hat{a}-\hat{a}^\dagger) + \frac{\hat{\mathbf{p}}^2}{2\mu} \\ &-\hbar\Delta_a\hat{\sigma}_+\hat{\sigma}_- - i\hbar g f(\hat{\mathbf{r}})(\hat{\sigma}_+\hat{a} - \hat{\sigma}_-\hat{a}^\dagger), \end{aligned} \tag{2}$$

where the terms on the right-hand side describe (from left to right)the cavity field, the pumping of the cavity, the atomic motion, the atomic internal energy, and the atom-field coupling; $\Delta_c = \omega_p - \omega_c$ and $\Delta_a = \omega_p - \omega_a$ are the cavity and atomic detunings from the frequency of the pumping laser, respectively; $\hat{a}$ and $\hat{a}^\dagger$ are the annihilation and creation operators of the cavity field, respectively; and $\hat{\sigma}_+$ and $\hat{\sigma}_-$ are the raising and lowering operators of the atom, respectively. The Liouvillian is given by [14]

$$\begin{aligned} \mathcal{L}\rho = \gamma &\left(2\int d^2\mathbf{u}N(\mathbf{u})\hat{\sigma}_- e^{-ik_a\mathbf{u}\cdot\hat{\mathbf{r}}}\rho e^{ik_a\mathbf{u}\cdot\hat{\mathbf{r}}}\hat{\sigma}_+ - [\hat{\sigma}_+\hat{\sigma}_-,\rho]_+\right) \\ &+ \kappa(2\hat{a}\rho\hat{a}^\dagger - [\hat{a}^\dagger\hat{a},\rho]_+), \end{aligned} \tag{3}$$

with $\mathbf{u}$ the direction vector of the spontaneously emitted photons and $N(\mathbf{u})$ the directional distribution for the atomic spontaneous emission, which is considered an isotropic one for simplicity; $k_a = \omega_a/c$ is the wave number corresponding to the atomic transition. The first term on the right-hand side of Eq. (3) describes the spontaneous emission together with the atomic momentum recoil, and the second term describes the cavity decay.

In our model, the atomic motion is restricted along the cavity axis (x direction in Fig. 1). The cavity-mode function is approximated by a sine mode $f(\hat{\mathbf{r}}) = f(\hat{x}) = \sin(K\hat{x})$, with

*xjzhou@pku.edu.cn

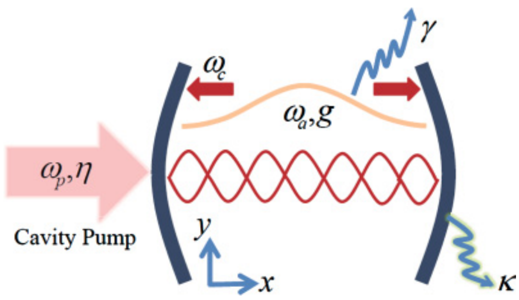

FIG. 1. (Color online) The cavity pump scheme. A two-level atom with transition frequency ω_a is coupled to a cavity with resonance frequency ω_c, which is coherently pumped by a laser with frequency ω_p and amplitude η. The coupling strength between the atom and the cavity is g. The cavity decay rate is 2κ and the atomic spontaneous emission rate is 2γ.

K the wave number of the cavity field. The recoil of the atom by spontaneously emitted photons is projected onto the cavity axis. The value of k_a can be well approximated by K since the detuning between the atomic transition frequency and the cavity resonance frequency is much smaller than ω_a and ω_c. The recoil frequency of the atom after either absorbing or emitting a photon from either the cavity field or the pump field is then presented as $\omega_r = \hbar K^2/(2\mu)$. Typical values of $\omega_r/(2\pi)$ for ^{133}Cs and ^{87}Rb are 2.0663 and 3.7710 kHz, respectively.

In the case of far-off-resonance pumping, the large atomic detuning leads to low atomic saturation, and we can adiabatically eliminate the upper atomic level. The lowering operator of the atom is then presented as [11,21]

$$\hat{\sigma}_- \approx \frac{g f(\hat{x})\hat{a}}{i\Delta_a - \gamma}, \tag{4}$$

and $\hat{\sigma}_+ = \hat{\sigma}_-^\dagger$. Inserting these expressions into Eqs. (2) and (3), we can obtain the effective Hamiltonian

$$H_{\text{eff}} = -\hbar\Delta_c \hat{a}^\dagger\hat{a} - i\hbar\eta(\hat{a} - \hat{a}^\dagger) + \frac{\hat{p}^2}{2\mu} + \hbar U_0 f^2(\hat{x})\hat{a}^\dagger\hat{a}, \tag{5}$$

and the effective Liouvillian

$$\mathcal{L}_{\text{eff}}\rho = \Gamma_0\left(2\sum_u N(u) f(\hat{x})\hat{a}e^{-iKu\hat{x}}\rho e^{iKu\hat{x}} - [f^2(\hat{x})\hat{a}^\dagger\hat{a},\rho]_+\right) + \kappa(2\hat{a}\rho\hat{a}^\dagger - [\hat{a}^\dagger\hat{a},\rho]_+), \tag{6}$$

with $U_0 = g^2\Delta_a/(\Delta_a^2 + \gamma^2)$ the effective atom-field coupling strength and $2\Gamma_0 = 2g^2\gamma/(\Delta_a^2 + \gamma^2)$ the effective spontaneous emission rate; u is the projection of the direction vector of the spontaneously emitted photons on the x axis. The cavity decay can be described by the jump operator $\hat{J}_c = \sqrt{2\kappa}\hat{a}$ and the spontaneous emission by the operator $\hat{J}_a = \sqrt{2\Gamma_0}e^{-iKu\hat{x}} f(\hat{x})\hat{a}$. The Liouvillian can be further transformed to the standard form $\mathcal{L}\rho = \sum_m (J_m\rho J_m^\dagger - \frac{1}{2}[J_m^\dagger J_m,\rho]_+)$.

The state vector of the system is given by $|\psi\rangle = \sum_{n,k} C_{n,k}(t)|n\rangle|k\rangle$, where $|n\rangle$ is the nth Fock state of the cavity field and $|k\rangle$ is the kth atomic momentum state, corresponding to a momentum $p = k\hbar K$. As in [6], the integration in Eq. (6) is reduced to the summation over $u = -1,0,1$. We assume the cavity field is in the vacuum state and the atom is in the zero-momentum state initially. Because of atomic momentum diffusion in the periodic potential, a very high dimension is needed for describing the momentum Hilbert space (in our simulation the dimension is taken to be 2^6). The Fock basis for the cavity field is truncated up to the 10th or 20th state. Using the Monte Carlo wave function method, we can simulate the time evolution for a stochastic trajectory of the state vector. According to the ergodic hypothesis, the dynamical process of the system can be expressed using the time-dependent density operator $\rho(t)$, which is given approximately by averaging over a large number of trajectories, and the steady-state properties of the system can be expressed by the steady-state density operator ρ_{ss}, which is approximated by averaging over a long time for one trajectory [6].

In order to show clearly the effects of the atomic spontaneous emission, we present results with and without spontaneous emission, respectively. The time evolution of the atomic momentum distribution, that is, the diagonal elements of $\rho(t)$, is plotted in Fig. 2. When the atomic spontaneous emission is neglected, the interference fringes in momentum space are formed with peaks at $p = 2m\hbar K(m = 0, \pm 1, \ldots)$ along with the establishment of the periodic potential in the cavity. Compared with the result of an optical lattice potential in free space [22], high-order momentum can be enhanced due to the strong atom-field coupling in the cavity.

When atomic spontaneous emission is considered, the recoil of the atom in random directions breaks the periodicity of the atomic spatial distribution. Thus, the spatial coherence of the atomic distribution is destroyed and the probability density

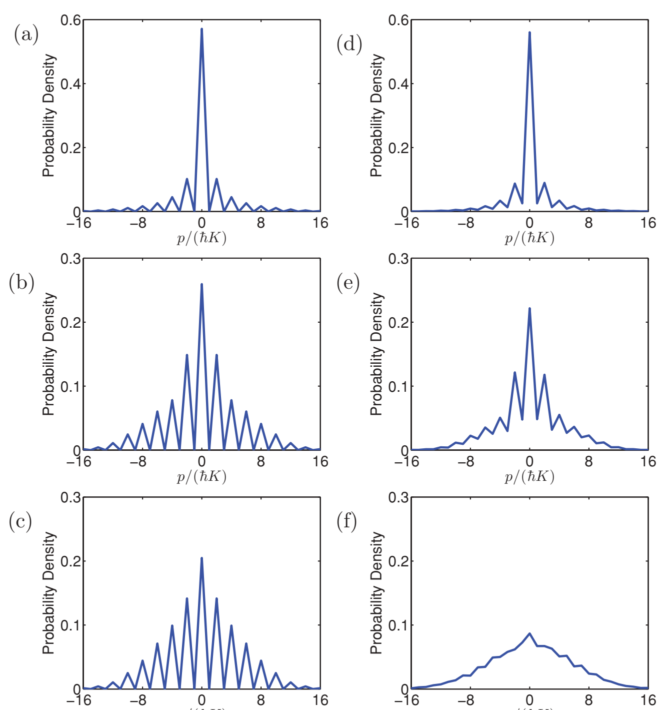

FIG. 2. (Color online) The atomic momentum distribution with (a)–(c) $\Gamma_0 = 0$ and (d)–(f) $\Gamma_0 = 18.75\omega_r$ for $\omega_r t = 0.032$, 0.16, and 0.72 from top to bottom. All results are given after averaging over 200 trajectories. The vertical axis represents the probability density, and $\kappa = 31.25\omega_r$, $\eta = 62.5\omega_r$, and $\Delta_c = U_0 = -390\omega_r$.

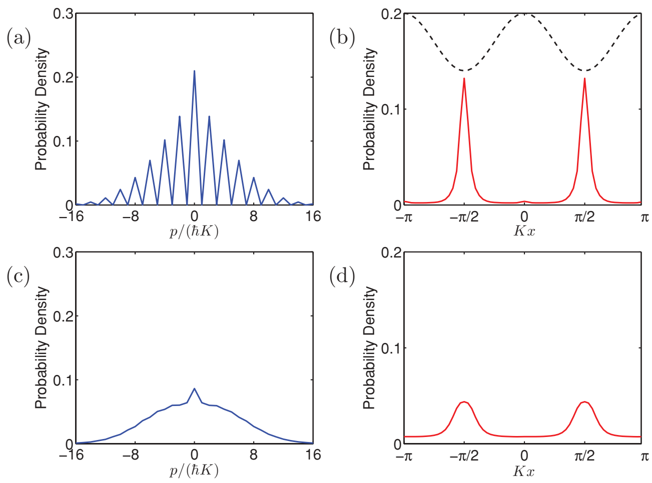

FIG. 3. (Color online) The probability density vs the atomic momentum and spatial distribution of the steady state: (a) atomic momentum and (b) spatial distribution for $\Gamma_0 = 0$, and (c) atomic momentum and (d) spatial distribution for $\Gamma_0 = 18.75\omega_r$. The dashed line in (b) shows the potential, and $\kappa = 31.25\omega_r$, $\eta = 62.5\omega_r$, and $\Delta_c = U_0 = -390\omega_r$.

is similar to a thermal equilibrium distribution. However, in the early stage of the establishment of the cavity field, because the spontaneous emission rate is much smaller than the atom-field coupling strength, the interference fringes can still be observed with lower visibility as shown by Figs. 2(d) and 2(e).

The spatial and momentum distributions for the steady state are given in Fig. 3. The peaks of the probability density are localized in the center of the lattice sites. When $\Gamma_0 = 0$, the coherence between different sites results in interference fringes in momentum space [see Fig. 3(a)]. Nevertheless, with notable atomic spontaneous emission, which may destroy the coherence among the sites, no fringes can be observed and the heating effect is depicted as shown in Fig. 3(c). In addition, with the same κ and η as well as nonzero Γ_0, the total decay rate is larger and the average photon number is smaller; thus, the peaks in Fig. 3(c) are smaller than in Fig. 3(a).

The atomic spatial coherence property can be measured by the coherence function $\chi(x)$ [6]:

$$\chi(x) = \int d(K\xi)|\rho_a(\xi,\xi + x)|, \tag{7}$$

where $\rho_a(x_1,x_2) = \langle x_1|(\sum_n \langle n|\rho|n\rangle)|x_2\rangle$ is the reduced density matrix describing the atomic spatial distribution. The coherence between neighboring sites is given by $\chi(x = \lambda_c/2 = \pi/K)$. The coherence function for different parameters is depicted in Fig. 4. When the spontaneous emission is neglected, the coherence between neighboring sites is conserved $[\chi(\pi/K) = 1]$. However, when the influence of spontaneous emission is considered, the coherence between neighboring sites vanishes $[\chi(\pi/K) \ll 1]$.

We can perform an integration for the coherence function to get the spatial coherence degree

$$C = \frac{1}{\pi}\int_0^{\pi} d(Kx)\chi(x), \tag{8}$$

which reflects the average coherence over a period of the atomic spatial distribution.

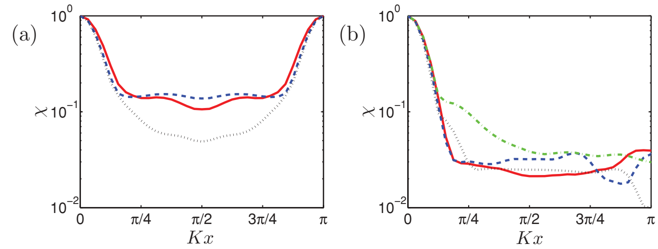

FIG. 4. (Color online) Atomic spatial coherence functions with (a) $\Gamma_0 = 0$ and (b) $\Gamma_0 = 18.75\omega_r$. The curves indicate different cavity decay rates and pumping amplitudes $(\kappa,\eta) = (0,31.25\omega_r)$, $(31.25\omega_r,31.25\omega_r)$, $(62.5\omega_r,31.25\omega_r)$, and $(31.25\omega_r,62.5\omega_r)$ shown as dash-dotted, solid, dashed, and dotted lines, respectively; $U_0 = \Delta_c = -390\omega_r$.

The time evolution of the atomic spatial coherence degree is shown in Fig. 5. With the establishment of the lattice in the cavity, the peaks for the probability density are localized in the center of the sites, and the nonuniform distribution leads to a decrease of the atomic spatial coherence. When the effect of spontaneous emission is considered, the phase of the atomic wave function at different sites is changed randomly due to the recoil, which may further decrease the coherence degree.

Now we investigate the influence of the cavity decay rate κ and the pumping amplitude η. From Eqs. (5) and (6) we know that the pumping amplitude and the cavity decay do not influence the atomic spatial or momentum distribution directly, but they influence the atom through the coupling term $\hbar U_0 f^2(\hat{x})\hat{a}^\dagger\hat{a}$. With large cavity decay, the cavity field adiabatically follows the atomic motion, and from the Heisenberg equation of $\hat{a}^\dagger$ and $\hat{a}$ we have

$$\hat{a}^\dagger\hat{a} = \frac{\eta^2}{\kappa^2 + [\Delta_c - U_0\sin^2(K\hat{x})]^2}. \tag{9}$$

Thus, even for the resonance situation of $\Delta_c = U_0$, the spatial spread of the atomic probability density still causes a shift of the cavity resonance frequency, which can be much larger than κ. Consequently, the cavity decay rate may have little influence on the atomic spatial distribution and the atomic coherence. Figures 4 and 5 show that the atomic coherence properties do not depend much on κ at fixed pumping strength η. However, for larger pumping strength η, the photon number in the cavity

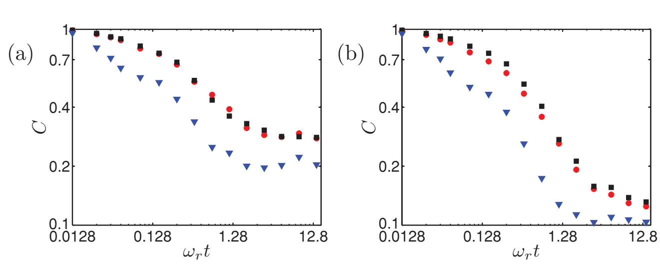

FIG. 5. (Color online) The time evolution of the atomic coherence degree with (a) $\Gamma_0 = 0$ and (b) $\Gamma_0 = 18.75\omega_r$. All results are given after averaging over 200 trajectories. The curves indicates different cavity decay rates and pumping amplitudes $(\kappa,\eta) = (0,31.25\omega_r)$, $(31.25\omega_r,31.25\omega_r)$, $(62.5\omega_r,31.25\omega_r)$, and $(31.25\omega_r,62.5\omega_r)$ shown as diamonds, circles, squares, and triangles, respectively; $\Delta_c = U_0 = -390\omega_r$.

is larger, resulting in a deeper potential for the optical lattice in the cavity. The peaks of the atomic spatial distribution become sharper, resulting in smaller coherence length. Therefore, the degree of atomic spatial coherence decreases.

The dynamics and steady-state properties for the atomic momentum and spatial distribution as well as the atomic spatial coherence have been investigated using the MCWF method. By comparing the results of situations with and without spontaneous emission, we find that the atomic spontaneous emission is dominant during the decoherence process. In addition, due to the atomic spatial spread of the probability distribution, the pumping strength is found to have greater influence on the photon number in the cavity and consequently the width of peaks in the atomic distribution, compared to the cavity decay rate. The spontaneous emission should be suppressed in experiments when the long-time evolution of the atomic spatial coherence is investigated. In fact, by normalizing the atomic wave function to the particle number N and modifying the effective coupling strength U_0 in Eq. (5) to the collective one NU_0, this model can also be used to investigate the coupling between a noninteracting Bose-Einstein condensate and the quantized cavity field. With the methods of absorption imaging and coherent measurement technology of cavity QED [23], the results may be directly observed and tested by experiments.

We are grateful to M. Z. Wu and T. Vogt for critically reading our manuscript. This work is partially supported by the state Key Development Program for Basic Research of China (Grants No. 2005CB724503, No. 2006CB921402, and No. 2006CB921401), NSFC (Grants No. 10874008 and No. 10934010), and SRF for ROCS and SEM.

[1] C. Maschler and H. Ritsch, Phys. Rev. Lett. **95**, 260401 (2005).
[2] P. Pinkse *et al.*, Nature (London) **404**, 365 (2002).
[3] V. Vuletić, H. W. Chan, and A. T. Black, Phys. Rev. A **64**, 033405 (2001).
[4] P. Maunz *et al.*, Nature (London) **428**, 50 (2004).
[5] S. Zippilli and G. Morigi, Phys. Rev. Lett. **95**, 143001 (2005).
[6] A. Vukics, J. Janszky, and P. Domokos, J. Phys. B **38**, 1453 (2005).
[7] H. Mabuchi *et al.*, Opt. Lett. **21**, 1393 (1996).
[8] I. B. Mekhov, C. Maschler, and H. Ritsch, Nature Phys. **3**, 319 (2007).
[9] I. B. Mekhov, C. Maschler, and H. Ritsch, Phys. Rev. Lett. **98**, 100402 (2007).
[10] C. Maschler *et al.*, Opt. Commun. **273**, 446 (2007).
[11] C. Maschler, I. B. Mekhov, and H. Ritsch, Eur. Phys. J. D **46**, 545 (2008).
[12] S. Slama, S. Bux, G. Krenz, C. Zimmermann, and P. W. Courteille, Phys. Rev. Lett. **98**, 053603 (2007).
[13] Xiaoji Zhou, Phys. Rev. A **80**, 023818 (2009).
[14] H. J. Carmichael, *Statistical Methods in Quantum Optics: Master Equations and Fokker-Planck Equations* (Springer, New York, 1999).
[15] J. Dalibard, Y. Castin, and K. Molmer, Phys. Rev. Lett. **68**, 580 (1992).
[16] C. W. Gardiner, A. S. Parkins, and P. Zoller, Phys. Rev. A **46**, 4363 (1992).
[17] A. Vukics and H. Ritsch, Eur. Phys. J. D **44**, 585 (2007).
[18] G. Lindblad, Commun. Math. Phys. **48**, 119 (1976).
[19] L. Allen and J. H. Eberly, *Optical Resonance and Two-Level Atoms* (Dover, New York, 1975).
[20] E. T. Jaynes and F. W. Cummings, Proc. IEEE **51**, 89 (1963).
[21] P. Meystre, *Atom Optics* (Springer, New York, 2001).
[22] M. Greiner *et al.*, Appl. Phys. B **73**, 769 (2001).
[23] D. F. Walls and G. J. Milburn, *Quantum Optics* (Springer-Verlag, Berlin, 1995).